

~~CONFIDENTIAL~~

Copy  
RM E54B09

NACA RM E54B09



# RESEARCH MEMORANDUM

PERFORMANCE CHARACTERISTICS OF SEVERAL SHORT ANNULAR  
DIFFUSERS FOR TURBOJET ENGINE AFTERBURNERS

By William E. Mallett and James L. Harp, Jr.

Lewis Flight Propulsion Laboratory  
Cleveland, Ohio

CLASSIFICATION CHANGED

UNCLASSIFIED

To \_\_\_\_\_

MAY 13 1954

By authority of \_\_\_\_\_ Date *Feb 26 1958*

*AMT 3-20 58*

CLASSIFIED DOCUMENT

This material contains information affecting the National Defense of the United States within the meaning of the espionage laws, Title 18, U.S.C., Secs. 793 and 794, the transmission or revelation of which in any manner to an unauthorized person is prohibited by law.

NATIONAL ADVISORY COMMITTEE  
FOR AERONAUTICS

WASHINGTON

May 13, 1954

~~CONFIDENTIAL~~



## NATIONAL ADVISORY COMMITTEE FOR AERONAUTICS

RESEARCH MEMORANDUM

## PERFORMANCE CHARACTERISTICS OF SEVERAL SHORT ANNULAR

## DIFFUSERS FOR TURBOJET ENGINE AFTERBURNERS

By William E. Mallett and James L. Harp, Jr.

## SUMMARY

Recent research has been directed toward the development of a short annular diffuser which would have low pressure loss and provide a uniform (flat) velocity profile at the diffuser exit. The performance characteristics reported herein were made in four short annular diffusers with different diffuser passage area variations and with various combinations of straightening vanes, vortex generators, splitters, and boundary layer suction for flow control.

Elimination of whirl (approximately  $20^\circ$  at the turbine discharge of the engine used for this investigation) provided the greatest single gain by reducing the tail-pipe pressure loss 2.4 percent, although with the elimination of whirl the flow separated severely from the curved inner body. The variation of diffusion rate investigated did not significantly change the tail-pipe pressure loss, although the diffuser exit velocity profile varied considerably. Splitters improved the profiles at the cost of 1 percent to 2.6 percent pressure loss. Vortex generators and boundary layer removal gave no improvement.

## INTRODUCTION

In order to realize the full potential of the turbojet-afterburner power plant, experience has shown that it is necessary to reduce the gas velocity efficiently from a Mach number as high as 0.8 at the turbine discharge to a Mach number of approximately 0.25 at the burner inlet. The diffuser in which the velocity reduction is accomplished must also provide a uniform (flat) velocity profile at the burner inlet, stable flow, and low pressure loss. The weight of the power plant, space for installation, and geometry of the system often lead to the use of a short annular diffuser.

The many problems associated with the diffusion process are familiar. The diffuser inlet conditions (radial and circumferential velocity distribution, boundary layer, direction of flow - nonaxial flow components) are critical. The adverse static pressure gradient that the main gas stream and boundary layer must overcome and the rate of geometric expansion are important. The over-all design problem becomes very complex because each of these and other problems are interrelated. References 1 to 6 and data not yet published, obtained by Wood and Higginbotham of the Langley laboratory, are a partial survey of recent research conducted to determine the performance of short annular diffusers.

The performance characteristics reported herein were made at the NACA Lewis laboratory as an integral part of a program to study the problems associated with the design and development of short afterburners for turbojet engines. During the program several types of diffusers were investigated. These included four different inner bodies with such flow regulating devices as straightening vanes, vortex generators, splitters, and boundary layer suction. Over-all configuration performance (tail-pipe pressure loss) and diffuser exit velocity profiles are presented.

#### APPARATUS

Engine. - The investigation was conducted on a production model, axial-flow, single-spool type turbojet engine with a nominal take-off rating of 5970 pounds of thrust with a rotor speed of 7950 revolutions per minute and with an exhaust gas temperature of 1275° F at sea-level, zero ram conditions. The engine has a 12-stage axial-flow compressor, eight cylindrical combustion chambers, and a single-stage turbine. Figure 1 is a diagram of the engine. The engine fuel used was MIL-F-5624A grade JP-4.

Engine installation. - The general arrangement of the engine installation is shown in figure 2. The engine was mounted on a swinging frame suspended from the ceiling of the test cell. The engine tail pipe extended through a diaphragm-type seal in the rear wall so that the exhaust gas was discharged into a sound-muffling chamber at approximately atmospheric pressure. The engine thrust was balanced and measured by a null-type air-pressure diaphragm. The greater portion of the engine combustion air was ducted from the atmosphere into the air-tight test cell and measured by a 26-inch, long-radius A.S.M.E. nozzle. The remainder of the combustion air was supplied by the laboratory high-pressure air system and entered the test cell through a single can-type combustor that was used to maintain the desired engine inlet-air temperature. Heating of the inlet air was accomplished by mixing the exhaust gas from the combustor with the atmospheric air. The heater air flow was metered with an A.S.M.E. flat-plate orifice.

Outer shells. - Two outer shell configurations were used during this investigation. The first (fig. 1(a)) was a standard production tail cone 28.44 inches long with four 16-inch-long inner body support struts. Connected to the tail cone were a straight pipe and convergent conical fixed-area exhaust nozzle, giving an over-all length of 54 inches. The second (fig. 1(b)) was the afterburner outer shell, which was designed to have the same over-all length required for the standard tail pipe. This afterburner outer shell was used for all configurations tested.

Diffuser configurations. - The twelve diffuser configurations reported herein consisted of the common afterburner outer shell and four inner bodies along with splitters, vortex generators, straightening vanes, and boundary layer suction in different combinations. The following paragraphs will describe each inner body and the devices tested with that particular inner body.

Curved inner body: The curved inner body along with the straightening vanes, splitter, and vortex generators tested with the curved inner body are shown in figure 3. A basic length of 18.17 inches and a blunt-end diameter of 12 inches (shown in fig. 3(a)) were selected for the inner body from considerations of diffusion and burning length requirements. The radius of curvature was selected to make the inner body parallel to the outer shell at the turbine discharge (to avoid a sudden change in radial flow direction out of the turbine) and to intersect the 12-inch diameter 18.17 inches downstream.

The straightening vanes, designed from references 7 and 8, were simple sheet metal, constant-curvature vanes constructed in two parts (to correct varying amounts of whirl across the passage). One part was welded to the outer shell and the other, to the inner body. The vane on the outer shell had a 0.5 inch span and a 2.5 inch chord. Figure 3(b) is a photograph of the straightening vane installation on the inner body.

The vortex generators, designed according to reference 2, were of simple sheet metal construction having a span of 0.5 inch and a chord of 2 inches. The 32 counter-rotating vortex generators, four sets of two in each quadrant between the inner body support struts, were equally spaced at the 30 percent chord line. In each set of two, one was positioned at  $+10^\circ$  and the other at  $-20^\circ$  with respect to the diffuser center line to orient them at an angle of attack of  $15^\circ$  with the measured flow angle.

The splitter was constructed of two conical sections welded together, and was designed to maintain approximately a constant area ratio between the inner and outer passages ( $A_0/A_1 = 1.174$ ).

Modified curved inner body: The second inner body investigated was the modified curved inner body shown in figure 4. The inner body length was held constant and the diameter of the blunt end increased from 12 to 16 inches. A conical section was constructed 16 inches in diameter at one end and increasing in diameter to a point where it became tangent to the previously described curved inner body. The forward part of the inner body remained intact with the straightening vanes in place. No auxiliary devices were tested with this inner body.

18-Inch straight inner body: The 18-inch straight inner body along with the splitter and two boundary layer suction systems investigated are shown in figure 5. Again the length of 18.17 inches and blunt-end diameter of 12 inches were held constant and a simple, easily manufactured conical inner body was constructed. The straightening vanes were of the same design as those for the curved inner body previously discussed.

A short splitter, formed by a series of sheet metal plates welded between the straightening vanes, was tested with the 18-inch straight inner body.

The turbine discharge boundary layer suction system consisted of 160 holes of 0.25-inch diameter drilled in the front face of the inner body near the outer surface, venting into an annular plenum chamber and on to the atmosphere in a duct extending through the exhaust nozzle.

The downstream suction system passed boundary layer air through a 1-inch wide slot, extending completely around the inner body, into a second annular plenum chamber, and on to the atmosphere as before.

24-Inch inner body: The fourth inner body investigated was the 24-inch inner body of figure 6. This inner body is a modified 18-inch straight inner body. The downstream 6 inches of the inner body were cut off and a 12-inch long conical section was welded in place. The blunt-end diameter of 12 inches was maintained. No auxiliary devices were tested with this inner body.

Each of the four inner bodies provided a diffuser which had a different area variation with length. Figure 7 shows the area variation for each of the inner body diffusers along with those for the diffusers of references 3 and 5. The diffusers of references 3 and 5 are also annular diffusers and will be discussed subsequently. The ordinate of the curve is the ratio of the diffuser area at any point to the diffuser inlet area. The abscissa is the ratio of the distance from the diffuser inlet to the radius of a circle of area equal to the diffuser inlet area; this ratio is used to generalize the curve and compare diffusers of different size directly. The sudden change in slope for diffusers A, B, and C at a length ratio of 1.107 is due to the shape of the outer shell.

Temperature and pressure instrumentation. - The locations of the instrumentation for temperature and pressure measurements are shown and the number of probes is tabulated in figure 1. Additional instrumentation is as follows:

- (a) Total pressure at engine inlet (station 0): two open-end tubes in quiescent regions of the test cell.
- (b) Static pressure at exhaust nozzle exit (station 9): average of three open-end tubes installed in the sound-muffling chamber in the plane of the exhaust nozzle exit.
- (c) Total temperature at bleed duct exit: average of two thermocouples at bleed duct exit.
- (d) Total pressure at bleed duct exit: average of three total pressure probes.
- (e) Static pressure at bleed duct exit: one wall static tap.
- (f) Total pressure, stream static pressure, and whirl angle at stations 6 and 7: one movable probe located at either station 6 or 7.

#### PROCEDURE

The performance data presented herein were obtained at static sea-level zero ram conditions with an engine inlet temperature of 100° F which was maintained by a combustion-type preheater when necessary. For each configuration data were obtained over a range of conditions from standard (engine speed, 7900 rpm; exhaust gas temperature, 1250° F) to 80 percent of standard (6400 rpm, 935° F). This corresponds to a diffuser inlet (turbine discharge) Reynolds number range of  $0.85 \times 10^6$  to  $0.79 \times 10^6$  based on the inlet hydraulic diameter and an inlet Mach number range of 0.6 to 0.5. At standard engine conditions the tail-pipe gas flow was 97 pounds per second at a pressure level of 3700 pounds per square foot. No flame holder or afterburner fuel spray bars were installed during the diffuser evaluation tests. Whirl data were taken at standard engine conditions to provide design data for and to determine the effectiveness of the straightening vanes. The exhaust gas temperature was measured at the exhaust nozzle exit where the gas was well mixed and an accurate average temperature could easily be obtained. The standard nonafterburning tail pipe (hereinafter called the standard tail pipe) was tested to provide a basis of comparison for the various diffuser configurations. The engine compressor efficiency was determined, as a measure of engine deterioration, and found to remain constant during this investigation.

## RESULTS AND DISCUSSION

The diffusers discussed herein are evaluated on the bases of diffuser exit velocity profile and pressure loss. The pressure loss, based on the total pressure available at the exhaust nozzle for the standard tail-pipe configuration, is shown in bar graph form in figure 8, which gives the ratio of exhaust nozzle exit total pressure for each configuration to the exhaust nozzle exit total pressure for the standard tail pipe at standard engine conditions of speed and exhaust gas temperature. This method of comparison was used because at standard engine conditions the diffuser inlet (turbine outlet) conditions were constant for all configurations tested; and because the inlet conditions were constant, this ratio provides an accurate measure of the diffuser losses relative to the standard tail pipe. The unpublished Langley data previously mentioned show that the use of a downstream total pressure gives an accurate measure of diffuser losses. A value of 95.8 percent on the bar graph in figure 8 (configuration B, for example) indicates a pressure loss 4.2 percent greater than the loss of the standard tail pipe. These values of pressure loss relative to the standard tail pipe are believed to be accurate within  $\pm 0.25$  percent. The loss of the standard tail pipe given in reference 9 is 4 percent of the turbine discharge total pressure.

## Turbine Discharge Whirl

As a result of turbine design and compressor development to increase turbojet engine air flow, whirl of various amounts often exists at the turbine outlet. The investigations reported in references 1, 3, and 5 discuss the effects of whirl on the performance of annular diffusers of the type with a constant-diameter outer shell and converging inner body. In order to maintain constant angular momentum through a diffuser of this type, an increase in the average angle of flow is required and the tangential component of kinetic energy is increased. The increase in whirl angle is not radially uniform, the largest angles (approaching  $90^\circ$ ) being near the inner wall. A radial static pressure gradient which assists divergence of the flow is established by centrifugal force which acts upon the air to create higher static pressures near the outer wall than near the inner wall; also, a centripetal flow of low-energy air, which is conducive to boundary layer separation, is established.

Reference 1 shows that the energy loss due to the rotation of flow is negligible at small inlet whirl angles and that the losses become significant at inlet whirl angles of  $20^\circ$  and larger. Reference 3 shows that the flow in the diffuser investigated separated from the inner body near the inlet for axial flow and an inlet whirl angle of  $15^\circ$ ; but that no flow separation occurred at an inlet whirl

angle of  $20^\circ$ . Reference 5 observed that flow separation from the inner body occurred farther downstream with  $20^\circ$  inlet whirl angle than with axial flow. Wood and Higginbotham concluded that for the best diffuser performance whirl should be eliminated from most of the gas stream, but that a particular amount of whirl, depending upon the diffuser geometry, was desirable near the inner body. The relation between the desirable amount of whirl and the diffuser geometry has not been defined.

Whirl existed at the turbine exit of the engine used for this investigation. The amount of whirl at two stations for the curved inner body diffuser is shown in figure 9. It can be observed that the whirl angle increased as the inner body radius decreased. The pressure and velocity profiles at the end of the diffuser inner body are shown in figure 10. The radial static pressure gradient established by the centrifugal force is clearly shown in figure 10(a), which gives the static and total pressure profiles across the passage. The velocity profile of figure 10(b) (computed from the local static to total pressure ratio and charts of ref. 10) indicates no flow separation and a relatively uniform velocity distribution compared with the other diffusers reported herein, which will be discussed. These measurements were made with a movable probe pointed directly into the flow and consequently are true stream values and not the axial component. The tail-pipe pressure loss of the curved inner body diffuser was 4.2 percent greater than the standard tail pipe, as shown in figure 8, configuration B.

Inasmuch as the diffuser is an intermediate part of a turbojet-afterburner power plant, the effect of whirl on afterburner performance must be considered in addition to the effect of whirl on diffuser performance. The energy associated with the rotational component of flow is lost for thrust purposes. Also, the axial velocity profile may be poor, depending on the amount and distribution of the whirl present. In addition to these undesirable characteristics, whirl may cause other detrimental effects during burning operation. References 11 and 12 adequately illustrate the harmful effects of whirl and benefits from eliminating whirl. Reference 12 reports that whirling flow separated from the inner body support struts providing undesirable flame seats upstream of the flame holder; after removal of the long strut fairings, the burning continued to be unstable. These undesirable effects were eliminated with the installation of flow straightening vanes. Reference 11 reports an increase of 3 percent to 7 percent in combustion efficiency, a decrease in pressure loss of 3 percent, and an increase in augmented net thrust ratio of 3 percent by eliminating turbine exit whirl.

Because of the high whirl angles (fig. 9) and the improvements in afterburner performance obtained with straightening vanes in references 11 and 12, the effect of straightening vanes at the turbine discharge



was investigated. The 37 straightening vanes (figs. 3(a) and 3(b)), designed in accordance with the linear relation of reference 7 and the correction of reference 8, were installed on the curved inner body. The effect of the straightening vanes on the whirl angle is shown in figure 11. The whirl was reduced to  $7^\circ$  or less at stations 6 and 7. At station 7 no data with straightening vanes were obtained within 4 inches of the inner body because the flow separated severely from the inner body. The effect of the straightening vanes on the pressure and velocity profiles at the end of the inner body is shown in figure 12. The velocity profile of figure 12(a) indicates no velocity in the region near the inner body and high velocity near the outer shell for the diffuser with straightening vanes as compared with the profile for whirl which indicated flow through the entire passage. Note that in figure 12(b) the static pressure is now nearly constant across the portion of the passage where flow exists. Six fixed rake total pressure tubes in the separated region recorded pressures, also shown, equal to or less than two outer wall static pressures and the stream static pressure.

With straightening vanes installed in the curved inner body diffuser the flow was approximately axial, and separated from the inner body when whirling flow did not. This phenomenon is unusual but is not unique, as discussed at the beginning of the RESULTS AND DISCUSSION section in connection with the work of references 3 and 5. As shown in figure 8, the tail-pipe pressure loss of the curved inner body diffuser with straightening vanes was only 1.8 percent greater than that of the standard tail pipe - a decrease in pressure loss of 2.4 percent from the curved inner body alone. In view of this net pressure increase and of the undesirable effects of whirl on afterburner performance which have been observed in other investigations, all subsequent inner bodies were equipped with straightening vanes.

#### Diffuser Passage Modification

Inner bodies. - In addition to the curved inner body, three other inner bodies with different rates of diffusion were investigated. The area variations (diffusion rates) for the four diffusers are presented in figure 7. The flow separation from the curved inner body with straightening vanes (hereinafter called the curved inner body) was undesirable because the velocity profile was not uniform and because, as indicated in references 12 and 13, separated regions may provide undesirable flame seats in the diffuser. In order to reduce the flow separation of the curved inner body diffuser, the rate of expansion was decreased by maintaining the length constant and increasing the diameter of the blunt end. A diagram of the modified curved inner body is given in figure 4. The change in the diffusion rate is shown in figure 7. The effect of the variation of diffusion rate on the

velocity profile at the end of the inner body (station 7) is presented in figure 13. The velocity profile at the end of the modified curved inner body is compared (fig. 13(a)) with the velocity profile for the curved inner body. The velocity profiles of figures 13 to 16 were computed from the ratio of outer wall static pressure (average of two static taps) to the stream axial total pressure (average of two fixed-rake total pressure tubes at each radial position) and the charts of reference 10. Very little change in the profile occurred with the change in area variation, although the flow separation was eliminated. The tail-pipe pressure loss (fig. 8, configuration D) was 1.2 percent greater than that of the standard tail pipe - a decrease in loss of 0.6 percent as compared with the curved inner body.

Preliminary exploratory runs prior to the investigation of the curved inner body indicated that a straight wall inner body might provide a better velocity profile than that obtained from the curved inner body; therefore the 18-inch straight inner body (fig. 5) was investigated more completely. As shown in figure 7, the diffusion rate differed widely from that of either the curved or modified curved inner bodies, although the sudden change in slope at a length ratio of 1.107 still existed. The velocity profile at the end of the 18-inch straight inner body diffuser (fig. 13(b)) was improved from that of the curved inner body (fig. 13(a)) in that the peak velocity was reduced and the separated region changed to a low velocity region. However, it should be noted that circumferential variations could exist and separation could occur near the inner body in a region where no instrumentation was located. The tail-pipe pressure loss was greater than the standard tail-pipe loss (fig. 8, configuration E) by 0.7 percent - a value less than that for either of the previous inner bodies.

In an effort to reduce the low velocity region near the surface of the 18-inch straight inner body and to provide a smooth diffusion rate, the 24-inch inner body (fig. 6) was constructed. The change in the slope of the area variation curve (fig. 7) at a length ratio of 1.107 was eliminated. As expected from the decrease in area at station 7, the velocities (fig. 13(b)) were increased across the passage. Any tendency of the flow to separate from the inner body was reduced with the increased velocity; however, the tail-pipe pressure loss (fig. 8) was 1.4 percent greater than that of the standard tail pipe - an increase of 0.7 percent from the 18-inch straight inner body.

The range of diffusion rates investigated did not provide a significant change in tail-pipe pressure loss. Note in figure 8 that the loss for configurations C, D, E, and F varies from 0.7 to 1.8 percent. There is little significant change in the diffuser exit velocity profiles; however, it is of interest to compare the profiles of the curved inner body and the 18-inch straight inner body. Each inner body had the same inlet, length, and outlet dimensions. The flow

3147

2-VB

separated from the curved inner body which had a low initial rate of expansion and an increasing rate of expansion with length. The flow did not separate from the 18-inch straight inner body which had a high initial rate of expansion and a generally decreasing rate of expansion with length. Thus it appears that the rate of geometric expansion affects the performance of diffusers with the same basic dimensions of length and area ratio.

Splitters. - The diffuser flow passages for the curved and 18-inch straight inner body diffusers were also varied by the installation of splitters. These splitters directed the flow toward the inner body and were intended to create more uniform profiles across the passage.

The long splitter investigated in conjunction with the curved inner body (shown in fig. 3(a)) was designed to maintain a constant area ratio between the outer and inner passages. The effect of splitters on the velocity profile at the end of the inner body is presented in figure 14. The velocity profile at the end of the curved inner body with the splitter is shown in figure 14(a) along with the profile for the curved inner body alone. The velocity in the outer passage was uniform and reduced to a level less than that of the curved inner body alone in the same region. The separation near the inner body was eliminated, giving an over-all profile that was relatively uniform; however, the tail-pipe pressure loss with the splitter was 1.0 percent greater than that for the curved inner body alone (fig. 8, configurations C and G).

In an attempt to reduce the splitter loss, the short splitter (shown in fig. 5) was designed for the 18-inch straight inner body. The splitter consisted of a series of plates welded between adjacent straightening vanes. The effect of the short splitter on the station 7 velocity profile is given in figure 14(b). The velocity, for unknown reasons (possibly due to a pressure fluctuation at the instant the data point was taken), was increased across the entire passage, although the profile shape was essentially unchanged. The addition of the splitter caused an increase in tail-pipe pressure loss (fig. 8, configurations E and H) of 2.6 percent.

Each splitter improved the diffuser exit velocity profile at the expense of additional tail-pipe losses; however, the splitters used do not necessarily represent an optimum design. Three splitter configurations were investigated in reference 14. Each of these splitters also improved the velocity profiles. Two gave additional tail-pipe losses of 1.5 and 2.8 percent; but the third decreased the loss by 0.7 percent.

## Boundary Layer Control

The effects of two boundary layer control devices, vortex generators and boundary layer suction, were investigated. The principle of the vortex generator is a re-energizing of the low-energy regions of the boundary layer with higher energy air through the vortex action of the tip of an airfoil. Boundary layer suction bleeds off the low-energy air, allowing higher-energy air to replace it.

Vortex generators. - The effect of vortex generators was investigated in conjunction with the curved inner body with and without the long splitter. The velocity profile changes were very slight, as can be seen in figure 15. More improvement due to the vortex generators was noted for the inner body alone (fig. 15(a)) than for the splitter configuration (fig. 15(b)). No change was recorded in tail-pipe pressure loss for either configuration (fig. 8, configurations C and I, G and J).

Boundary layer suction. - The inner body boundary layer downstream of the turbine may contain low energy air from two sources: the flow through the turbine near the blade roots, and the air used to cool the rear face of the turbine wheel. (The cooling air may be discharged, as in this engine, perpendicular to the gas stream through a small clearance space between the upstream end of the inner body and the turbine wheel.) These low-energy flows tend to aggravate the already severe problem of keeping the flow from separating. The effects of bleeding off boundary layer air at two locations on the inner body were investigated in conjunction with the 18-inch straight inner body diffuser.

In order to bleed low-energy air from the diffuser as near the source as possible, the turbine discharge bleed system was installed. The bleed system (shown in fig. 5) passed air through a series of holes drilled in the front face of the inner body near the outer surface and vented to a plenum chamber. The plenum chamber was vented to atmosphere through a duct extending out of the exhaust nozzle. Different quantities of air from 0 to 1.4 percent of the engine air flow were bled off through this system. The turbine cooling air amounted to only 0.25 percent of the engine air flow. No auxiliary power was required for the bleed system since the air flowed from a region inside the engine to a lower pressure region outside the engine. The air flow was metered through a flat-plate orifice in the bleed duct. The effect of the turbine discharge boundary layer suction on the velocity profile is shown in figure 16. The turbine discharge bleed system did not improve the velocity profile (fig. 16), and the tail-pipe pressure loss was increased by 0.6 percent from that of the 18-inch straight inner body alone (fig. 8, configurations E and K).

The second bleed system (fig. 5) consisted of a 1-inch-wide slot, extending completely around the inner body, located 8 inches downstream of the turbine discharge. The slot vented into an annular plenum chamber and on to the atmosphere as before. Again different quantities of air were bled off (0 to 2.2 percent of the engine air flow) through the system. The tail-pipe pressure loss (fig. 8, configurations L and M) for both 0 and 2.2 percent bleed was 0.6 percent greater than that of the 18-inch straight inner body. The pressure measurements at station 7 with this configuration were unreliable and, therefore, velocity profiles are not presented.

#### SUMMARY OF RESULTS

As an integral part of a program to study the problems associated with the design and development of short afterburners for turbojet engines, twelve diffuser configurations were investigated to determine the effect of straightening vanes, diffusion rate variation, splitters, vortex generators, and boundary layer suction on the tail-pipe pressure loss and diffuser exit velocity profiles.

Elimination of whirl (approximately  $20^\circ$  at turbine discharge) provided the greatest single gain in diffuser performance obtained in this investigation by reducing the tail-pipe pressure loss of the curved inner body diffuser by 2.4 percent; however, with the elimination of whirl the flow separated severely from the curved inner body.

For the diffusers investigated, changes in the diffusion rate did not significantly change the tail-pipe pressure loss (0.7 to 1.8 percent), although the diffuser exit velocity profiles varied considerably. The flow in the curved inner body diffuser separated while the flow in the 18-inch straight inner body diffuser did not.

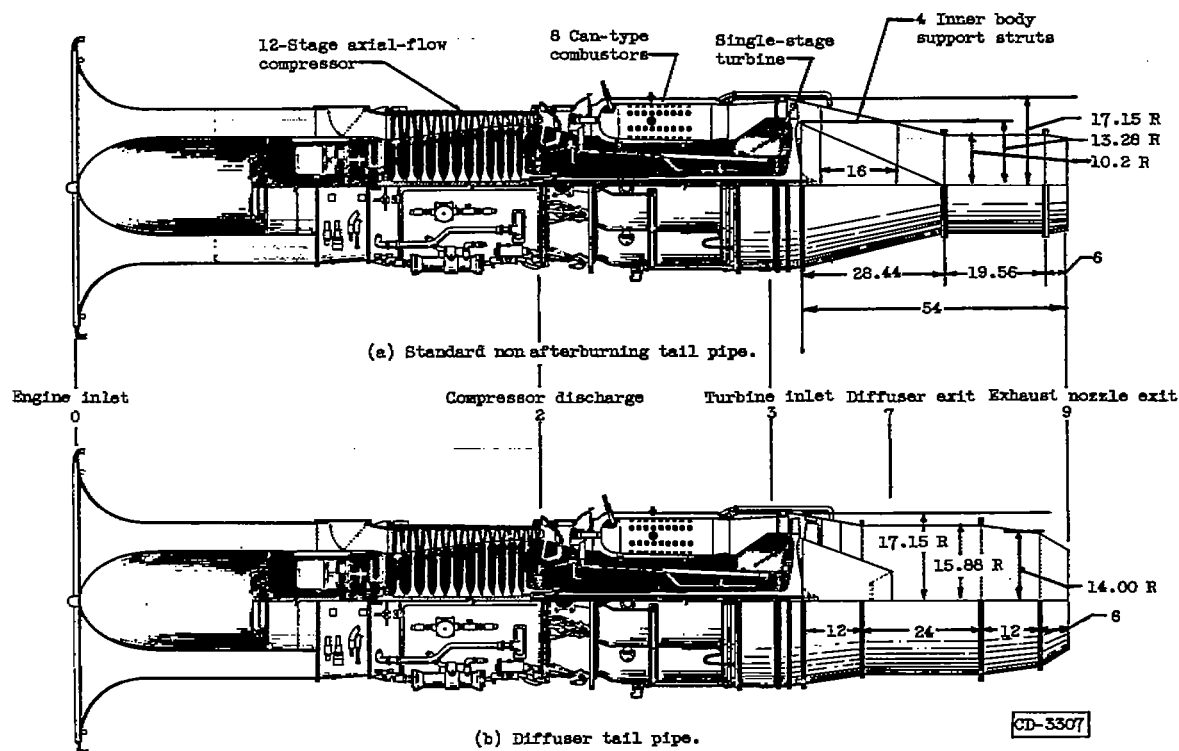
The addition of splitters improved the diffuser exit velocity profiles at the cost of 1 to 2.6 percent increased tail-pipe pressure loss. The addition of vortex generators and boundary layer suction at the turbine discharge did not alter the velocity profiles but caused a slight loss in tail-pipe pressure.

Lewis Flight Propulsion Laboratory  
National Advisory Committee for Aeronautics  
Cleveland, Ohio, February 16, 1954

## REFERENCES

1. Schwartz, Ira A.: Investigation of an Annular Diffuser-Fan Combination Handling Rotating Flow. NACA RM L9B28, 1949.
2. Wood, Charles C.: Preliminary Investigation of the Effects of Rectangular Vortex Generators on the Performance of a Short 1.9:1 Straight-Wall Annular Diffuser. NACA RM L51G09, 1951.
3. Wood, Charles C., and Higginbotham, James T.: The Influence of Vortex Generators on the Performance of a Short 1.9:1 Straight-Wall Annular Diffuser with a Whirling Inlet Flow. NACA RM L52L01a, 1953.
4. Wood, Charles C., and Higginbotham, James T.: Flow Diffusion in a Constant-Diameter Duct Downstream of an Abruptly Terminated Center Body. NACA RM L53D23, 1953.
5. Wood, Charles C., and Higginbotham, James T.: Performance Characteristics of a  $24^\circ$  Straight-Outer-Wall Annular-Diffuser-Tailpipe Combination Utilizing Rectangular Vortex Generators for Flow Control. NACA RM L53H17a, 1953.
6. Henry, John R., and Wilbur, Stafford W.: Investigation of the Flow in an Annular-Diffuser-Tailpipe Combination with an Abrupt Area Expansion and Suction, Injection, and Vortex-Generator Flow Controls. NACA RM L53K30, 1954.
7. Lieblein, Seymour: Turning-Angle Design Rules for Constant-Thickness Circular-Arc Inlet Guide Vanes in Axial Annular Flow. NACA TN 2179, 1950.
8. Lieblein, Seymour, and Sandercock, Donald M.: Compressibility Correction for Turning Angles of Axial-Flow Inlet Guide Vanes. NACA TN 2215, 1950.
9. Renas, Paul E., and Jansen, Emmert T.: Altitude Performance Characteristics of the J47-25 Turbojet Engine - Data Presentation. NACA RM E52G22, 1953.
10. Turner, L. Richard, Addie, Albert N., and Zimmerman, Richard H.: Charts for the Analysis of One-Dimensional Steady Compressible Flow. NACA TN 1419, 1948.
11. Braithwaite, Willis M., Walker, Curtis L., and Sivo, Joseph N.: Altitude Evaluation of Several Afterburner Design Variables on a J47-GE-17 Turbojet Engine. NACA RM E53F10, 1953.

12. Braithwaite, Willis M., Renas, Paul E., and Jansen, Emmert T.:  
Altitude Investigation of Three Flame-Holder and Fuel-Systems  
Configurations in a Short Converging Afterburner on a Turbojet  
Engine. NACA RM E52G29, 1952.
13. Fleming, W. A., Conrad, E. William, and Young, A. W.: Experimental  
Investigation of Tail-Pipe-Burner Design Variables. NACA RM  
E50K22, 1951.
14. Conrad, E. William, Schulze, Frederick W., and Usow, Karl H.:  
Effect of Diffuser Design, Diffuser-Exit Velocity Profile, and  
Fuel Distribution on Altitude Performance of Several Afterburner  
Configurations. NACA RM E53A30, 1953.



Station	Pressure and temperature instrumentation					
	Standard tail pipe			Diffuser tail pipe		
	Thermocouples	Total pressures	Static pressures	Thermocouples	Total pressures	Static pressures
0	20	0	0	20	0	0
2	24	24	4	24	24	4
3	8	8	0	8	8	0
7	0	0	0	0	16	2
9	14	14	0	14	14	0

Figure 1. - Engine diagram and instrumentation. (All dimensions are in inches.)



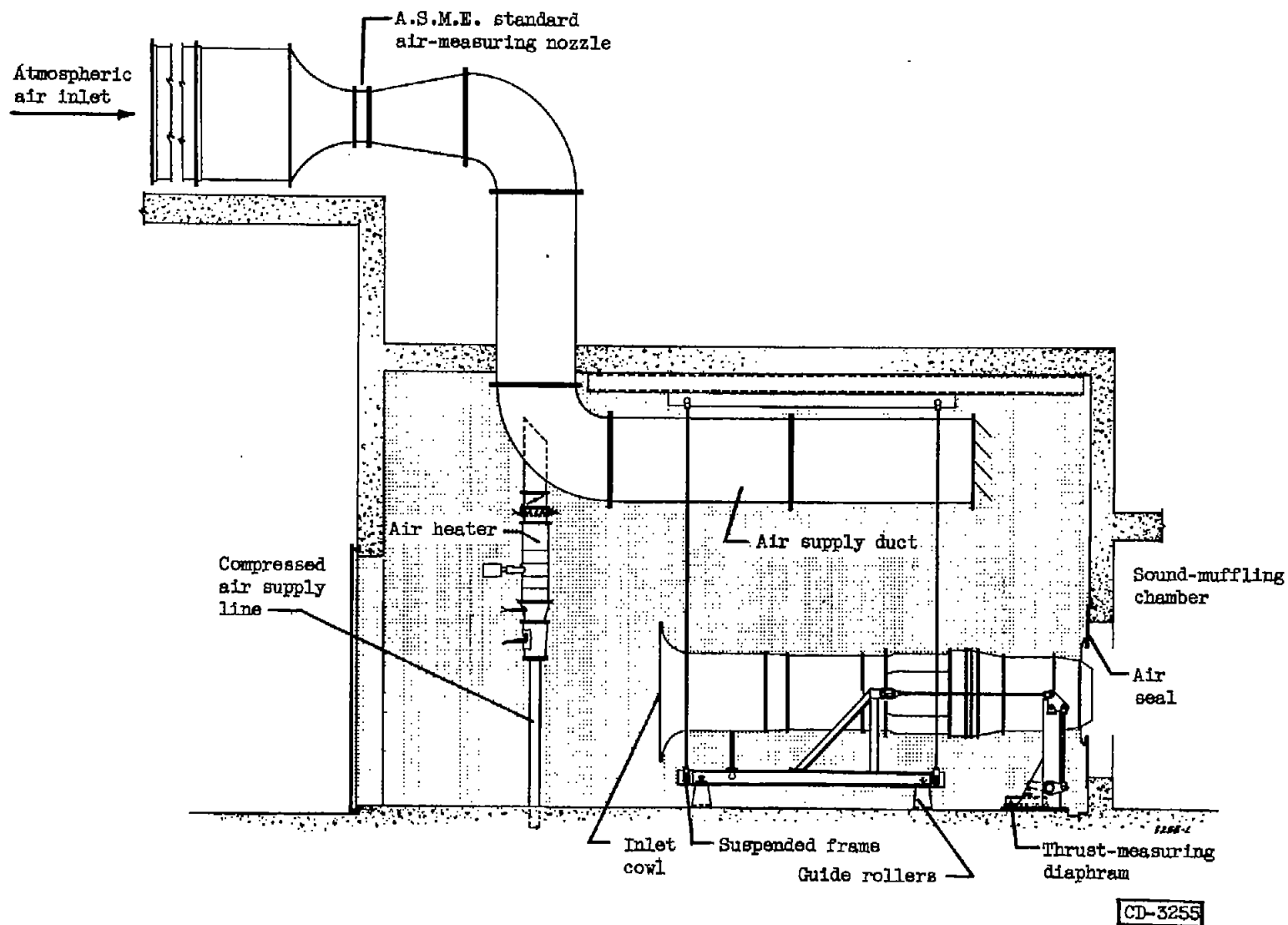
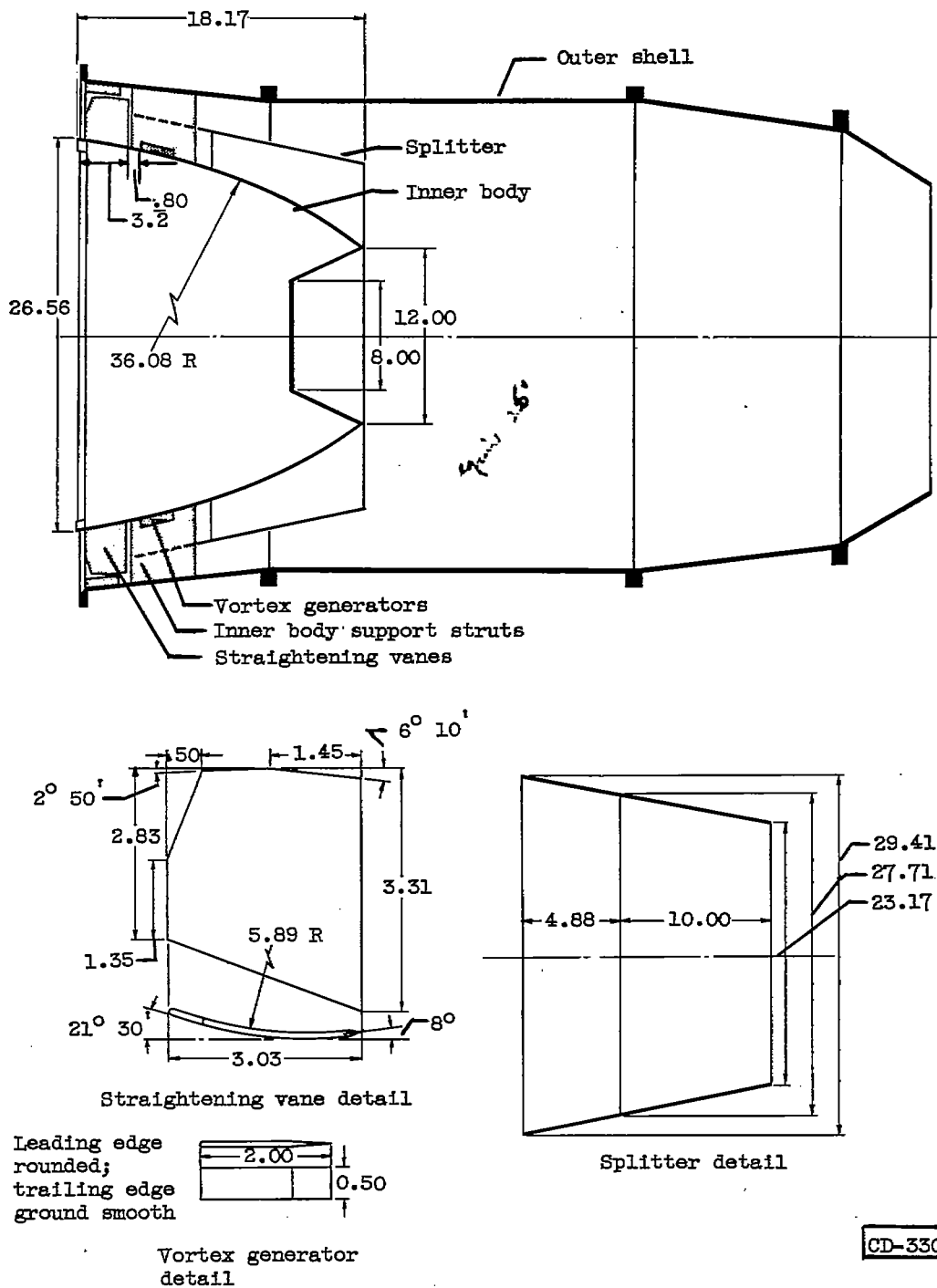


Figure 2. - Schematic diagram of engine installation.



(a) Diagram showing straightening vanes, vortex generators, and splitter.

Figure 3. - Curved inner body. (All dimensions are in inches.)



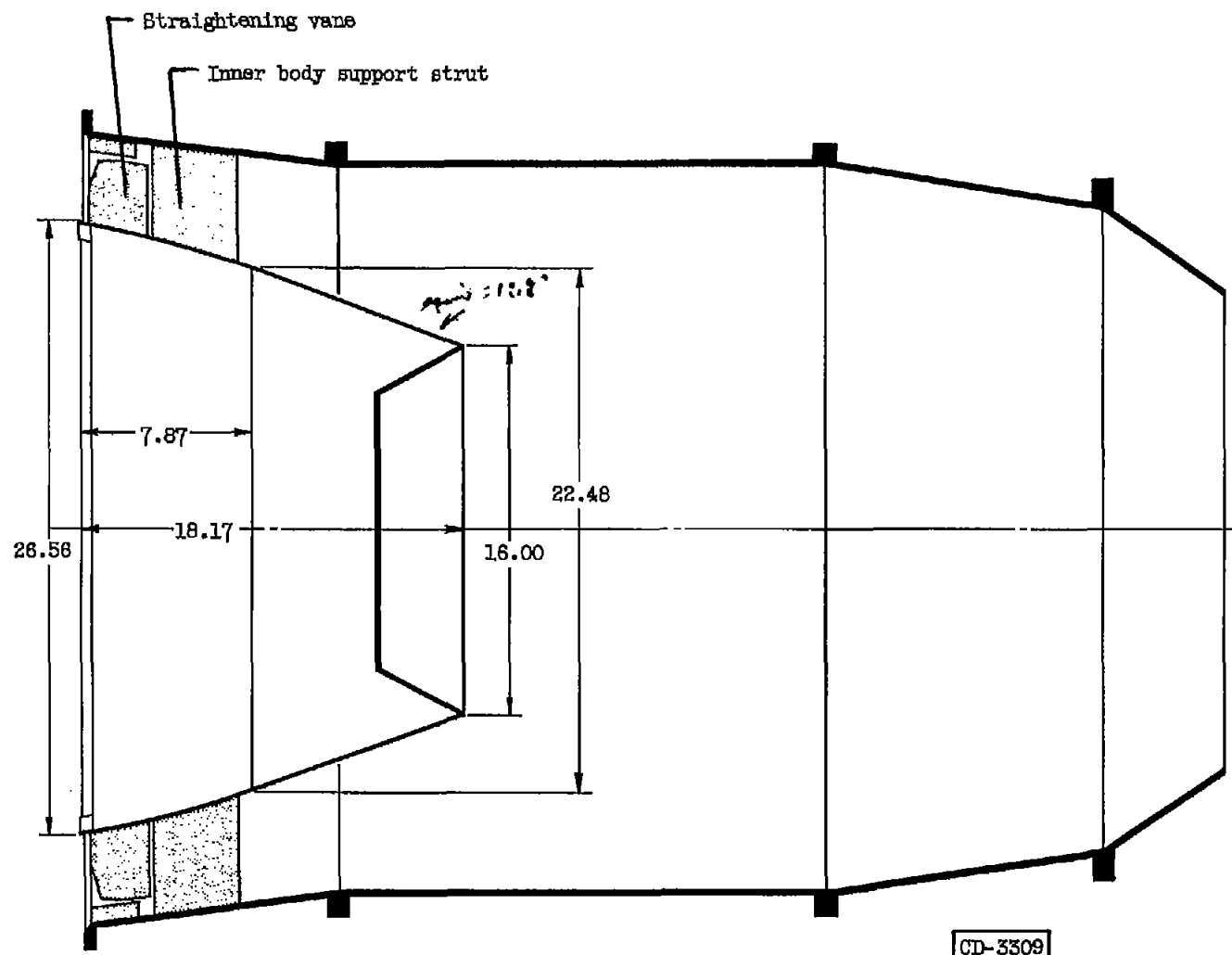


Figure 4. - Modified curved inner body with straightening vanes. (All dimensions are in inches.)

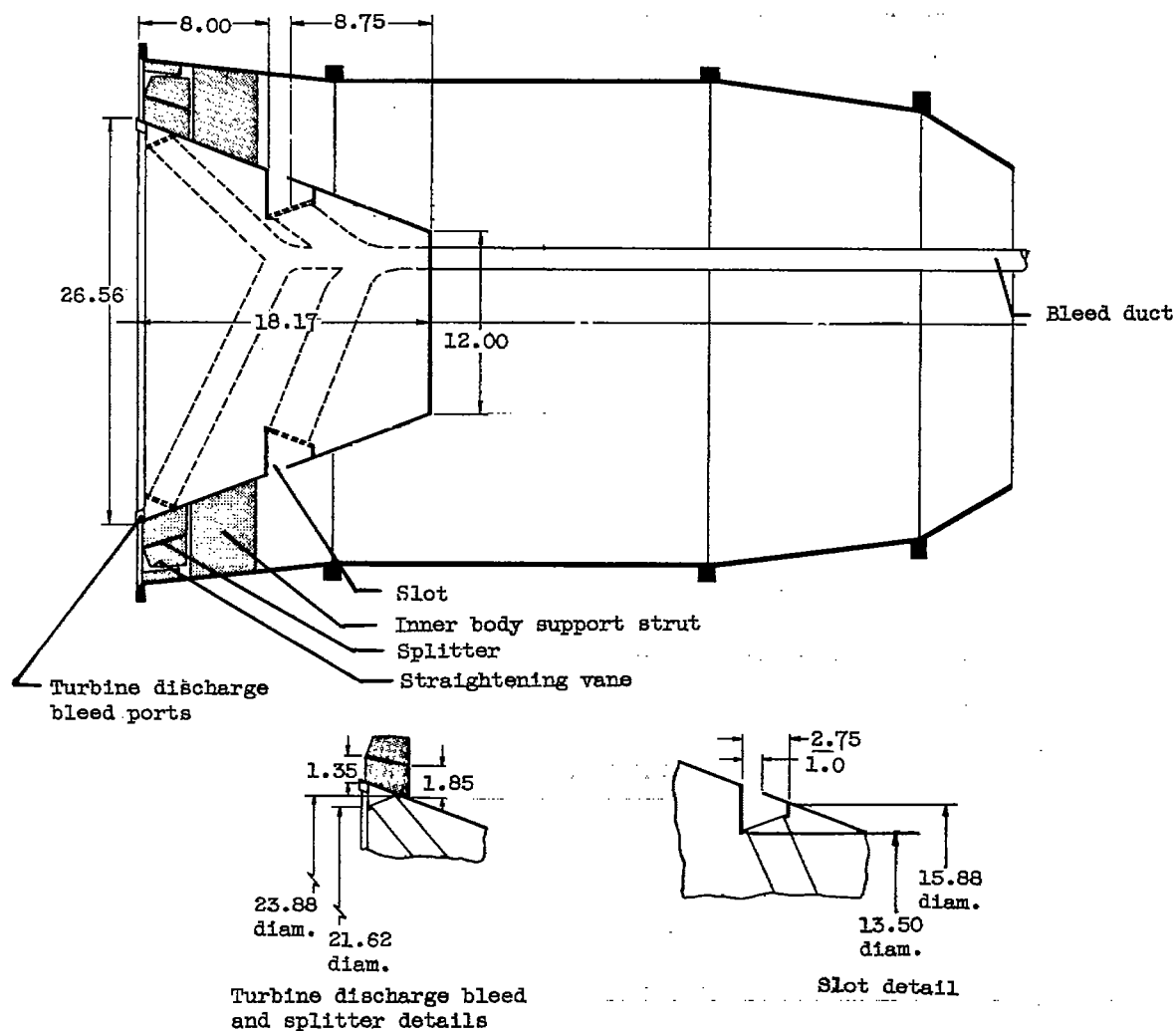


Figure 5. - 18-Inch straight inner body with straightening vanes, splitter, and bleed facilities. (All dimensions are in inches.)

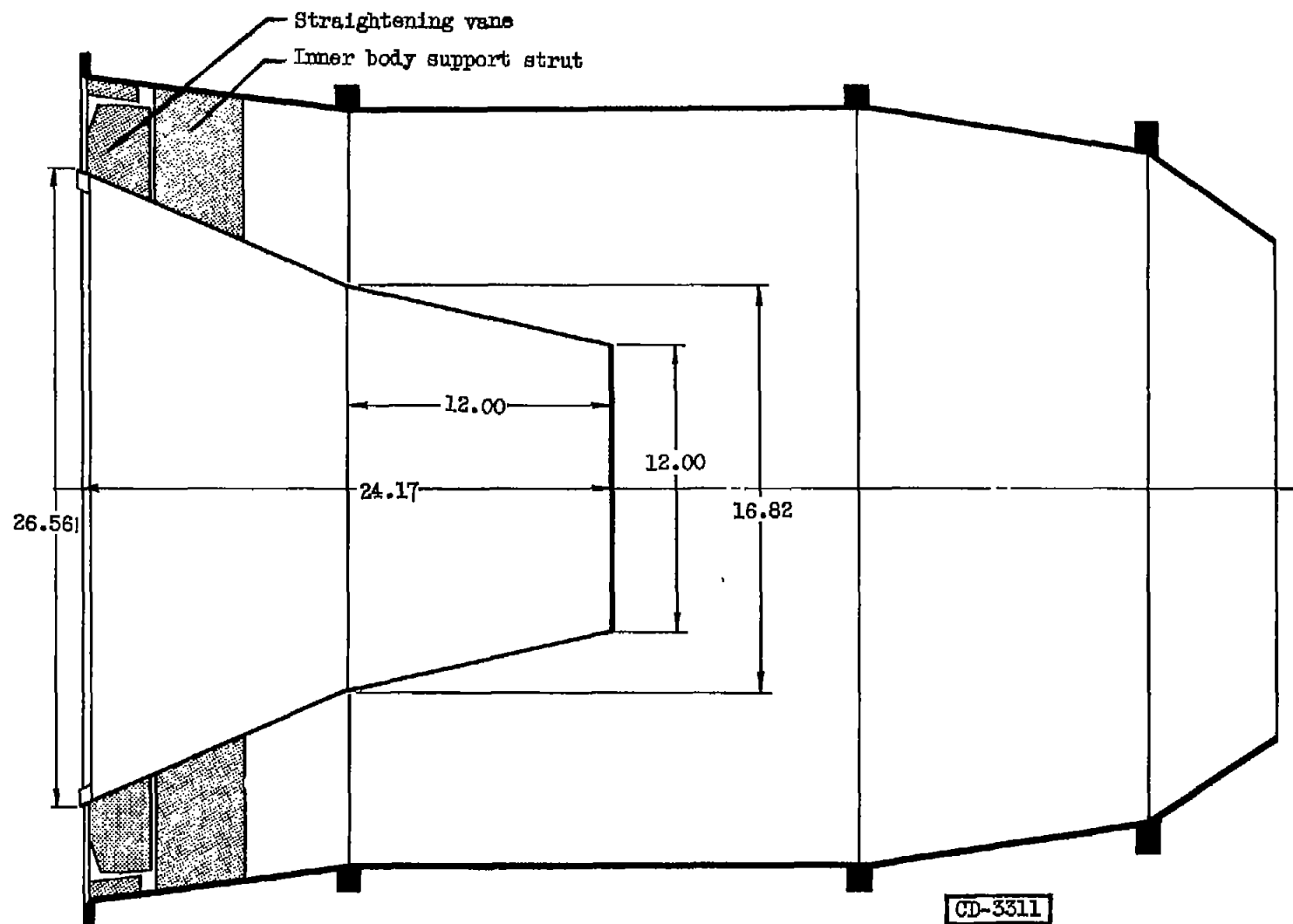


Figure 6. - 24-Inch inner body with straightening vanes. (All dimensions are in inches.)

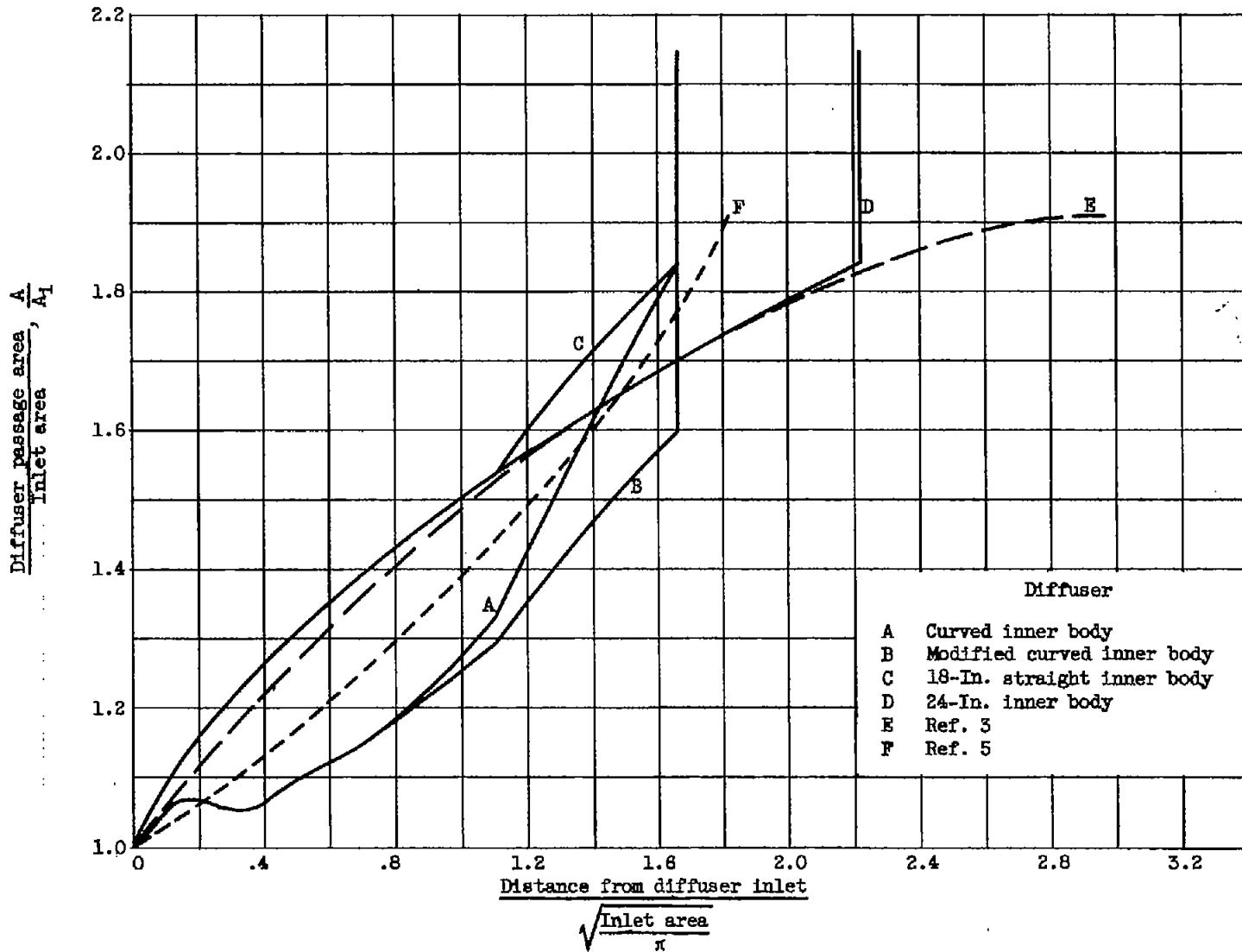


Figure 7. - Diffuser area variation with length ratio.

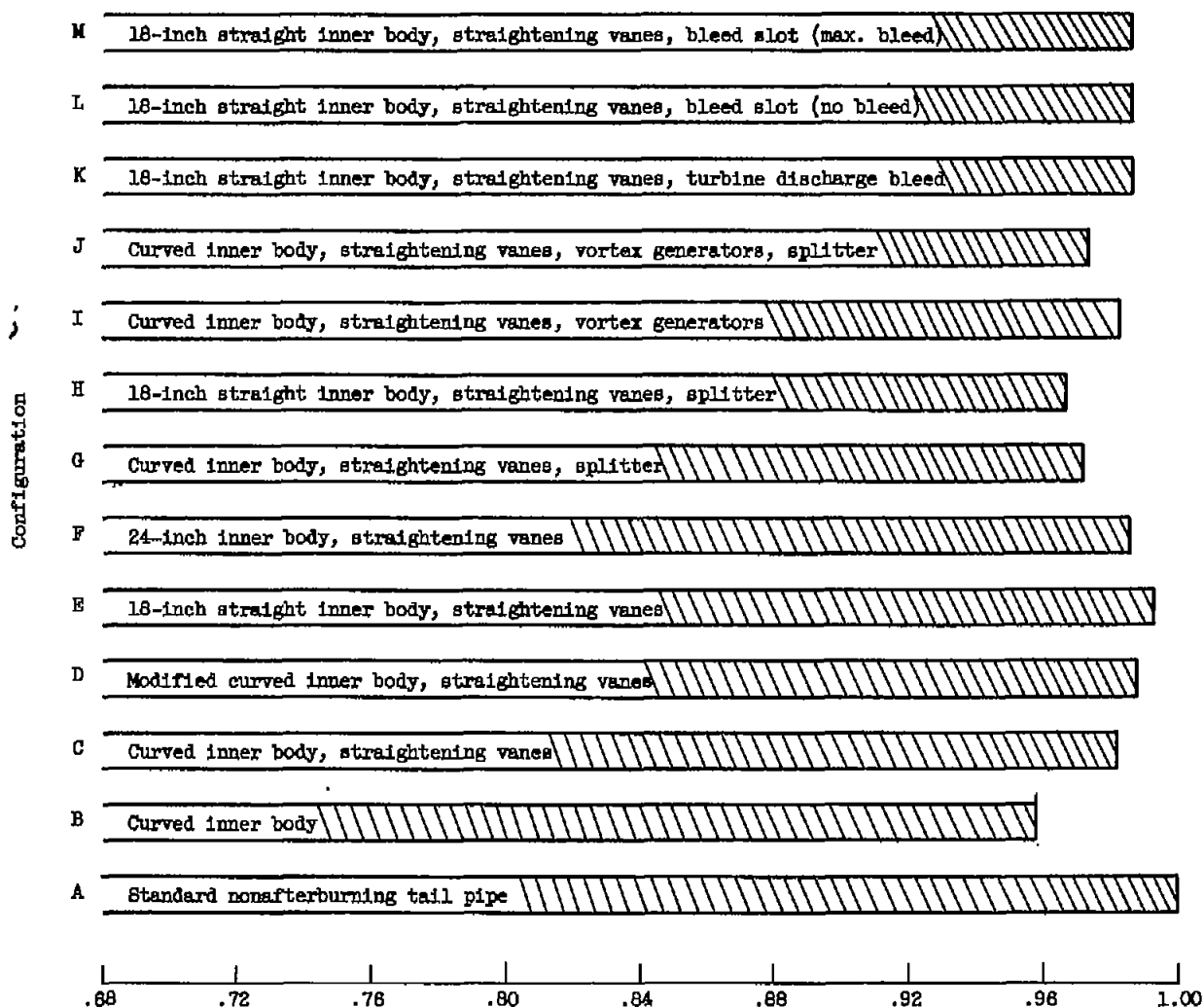


Figure 8. - Ratio of exhaust nozzle total pressure for NACA diffuser configurations to exhaust nozzle total pressure for standard nonafterburning tail pipe. Engine speed, 7900 rpm; inlet temperature, 560° R; engine temperature ratio, 3.055.



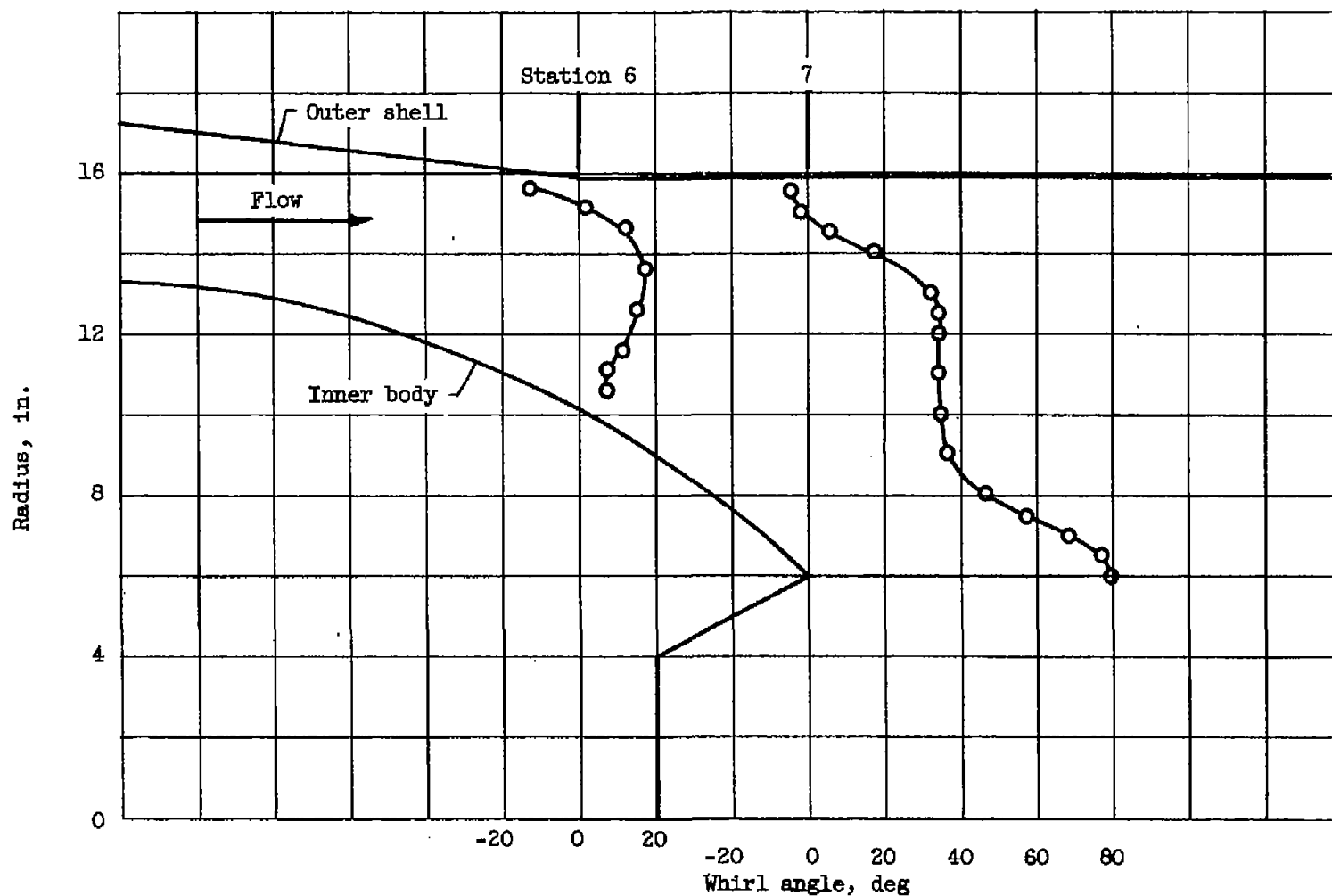


Figure 9. - Whirl profiles for curved inner body diffuser. Engine speed, 7900 rpm; inlet temperature,  $100^{\circ}\text{F}$ ; exhaust gas temperature,  $1250^{\circ}\text{F}$ . Positive whirl is opposite turbine rotation.

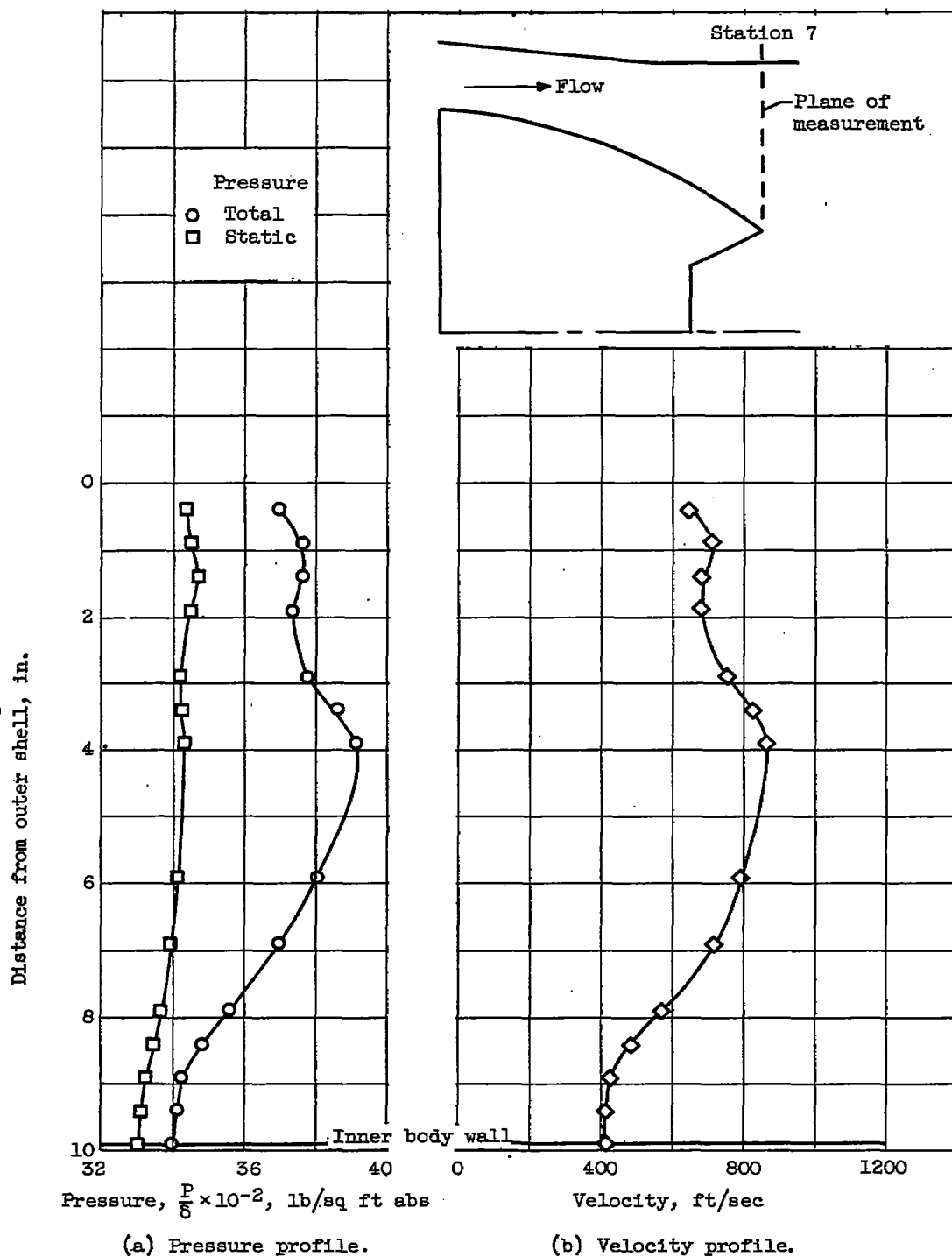


Figure 10. - Pressure and velocity profiles at end of curved inner body diffuser. Engine speed, 7900 rpm; inlet temperature, 100° F; exhaust gas temperature, 1250° F.

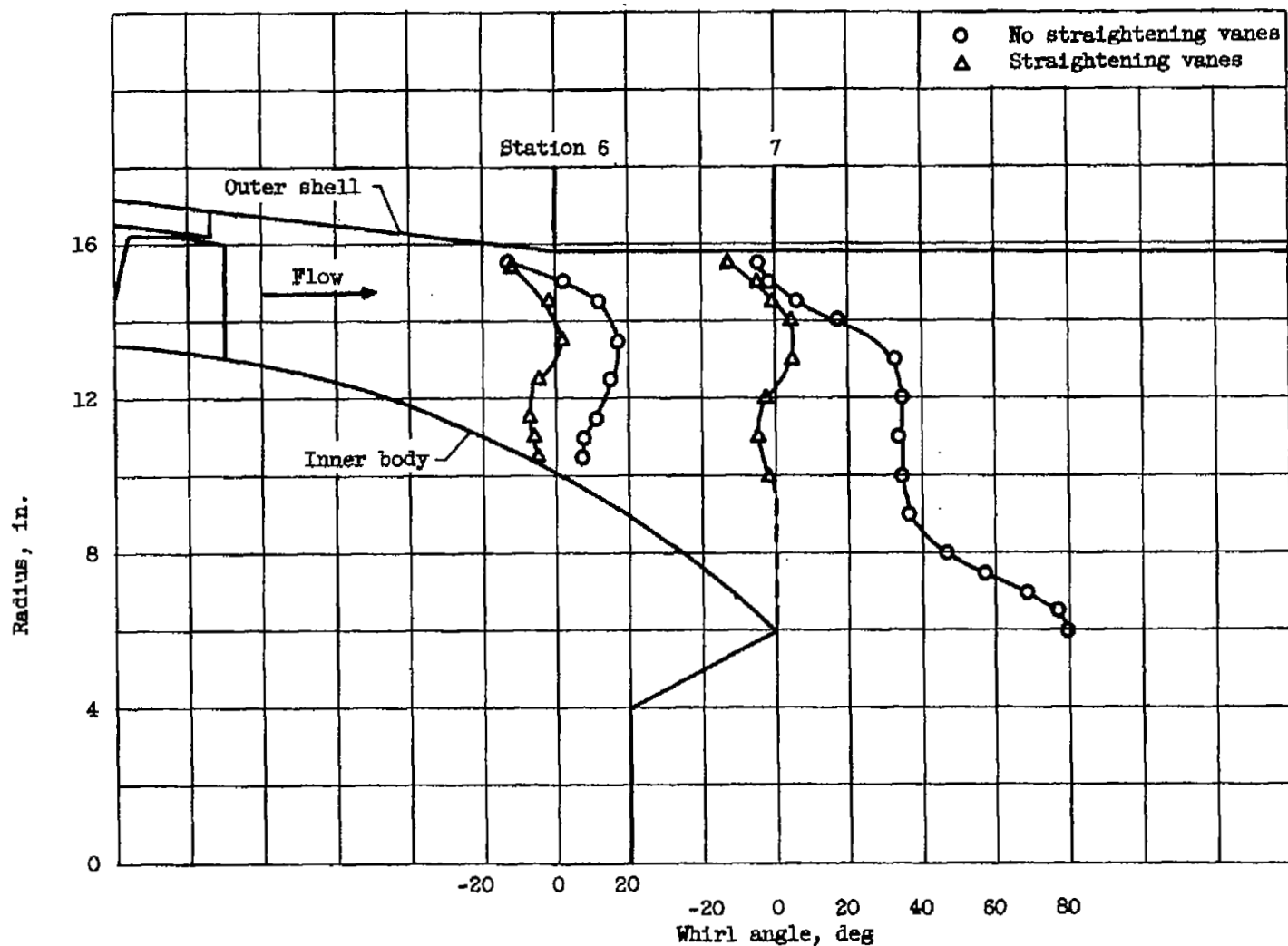


Figure 11. - Effect of straightening vanes on whirl profiles for curved inner body diffuser. Engine speed, 7900 rpm; inlet temperature, 100° F; exhaust gas temperature, 1250° F. Positive whirl is opposite turbine rotation.

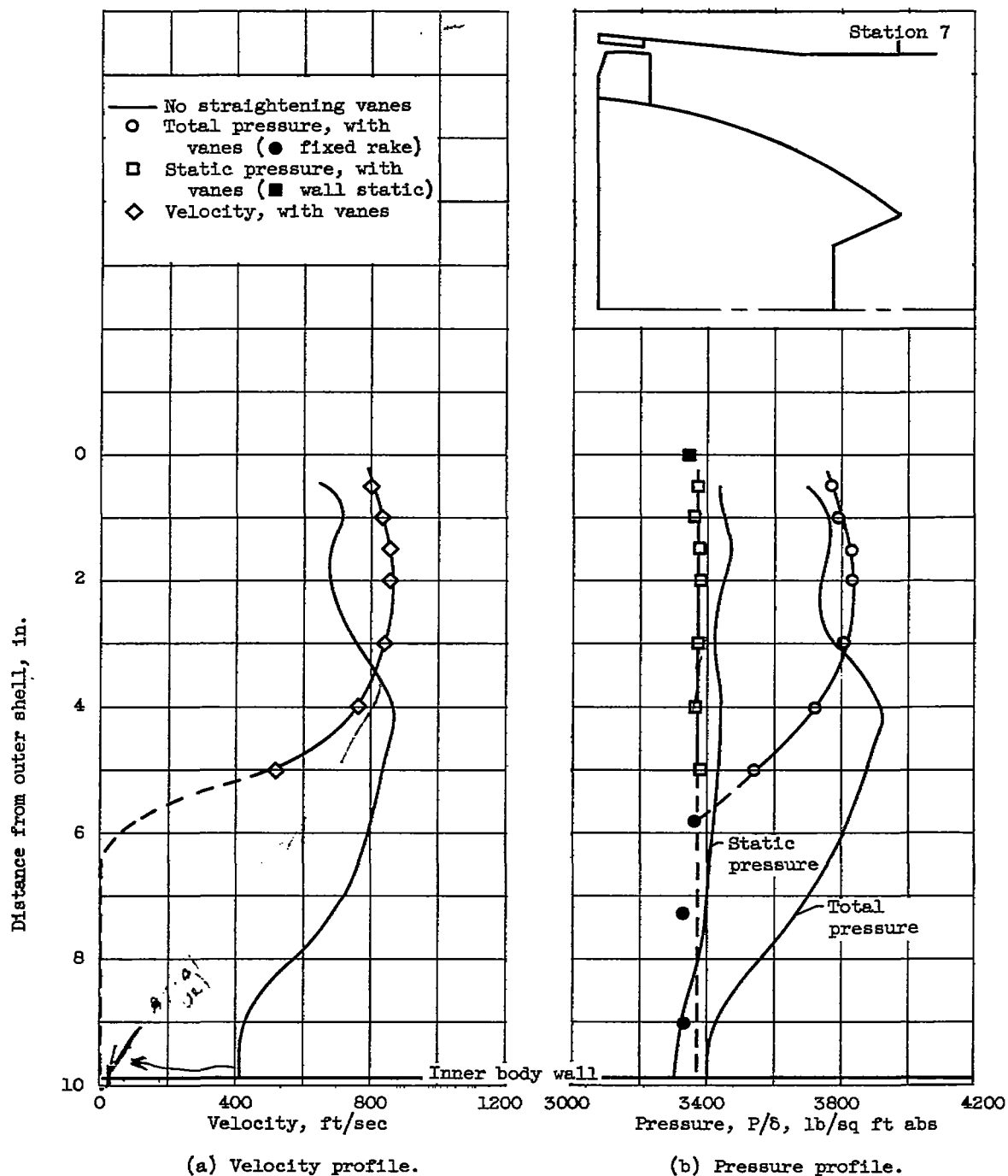
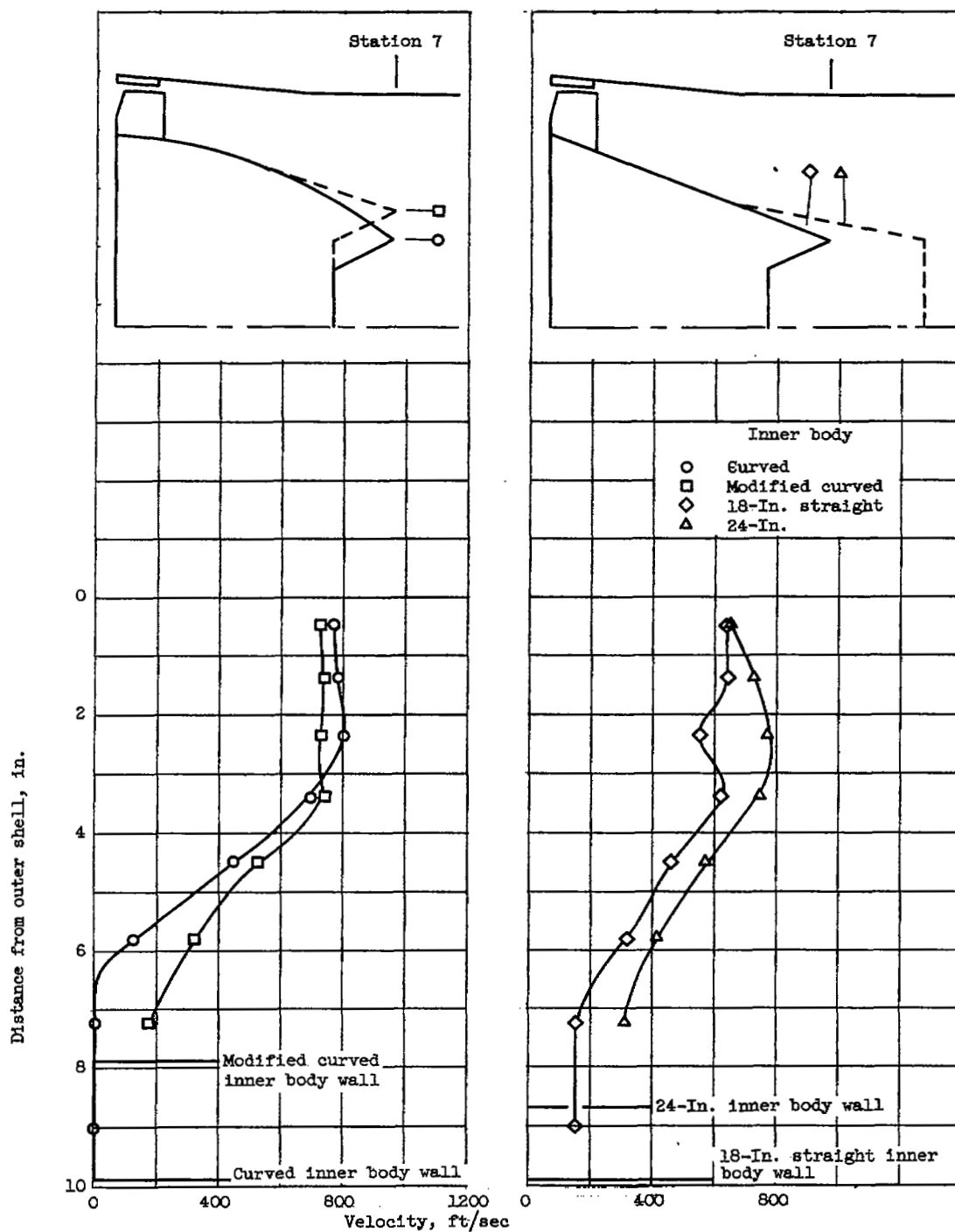


Figure 12. - Effect of straightening vanes on pressure and velocity profiles at end of curved inner body diffuser. Engine speed, 7900 rpm; inlet temperature, 100° F; exhaust gas temperature, 1250° F.



(a) Curved and modified curved inner bodies.

(b) 18-inch straight and 24-inch inner bodies.

Figure 13. - Effect of diffuser area variation on velocity profile at station 7.  
Engine speed, 7900 rpm; inlet temperature, 100° F; exhaust gas temperature, 1250° R.

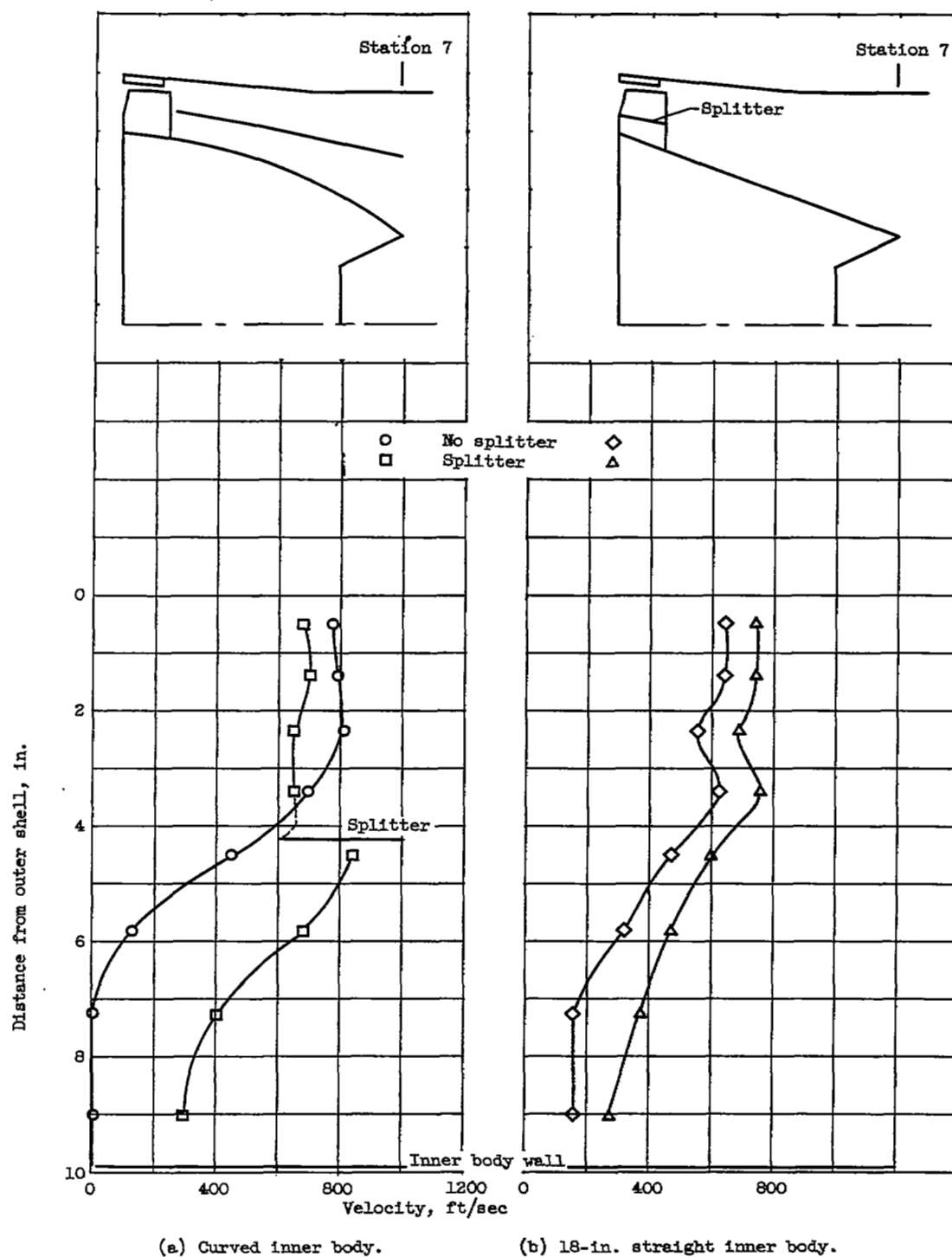
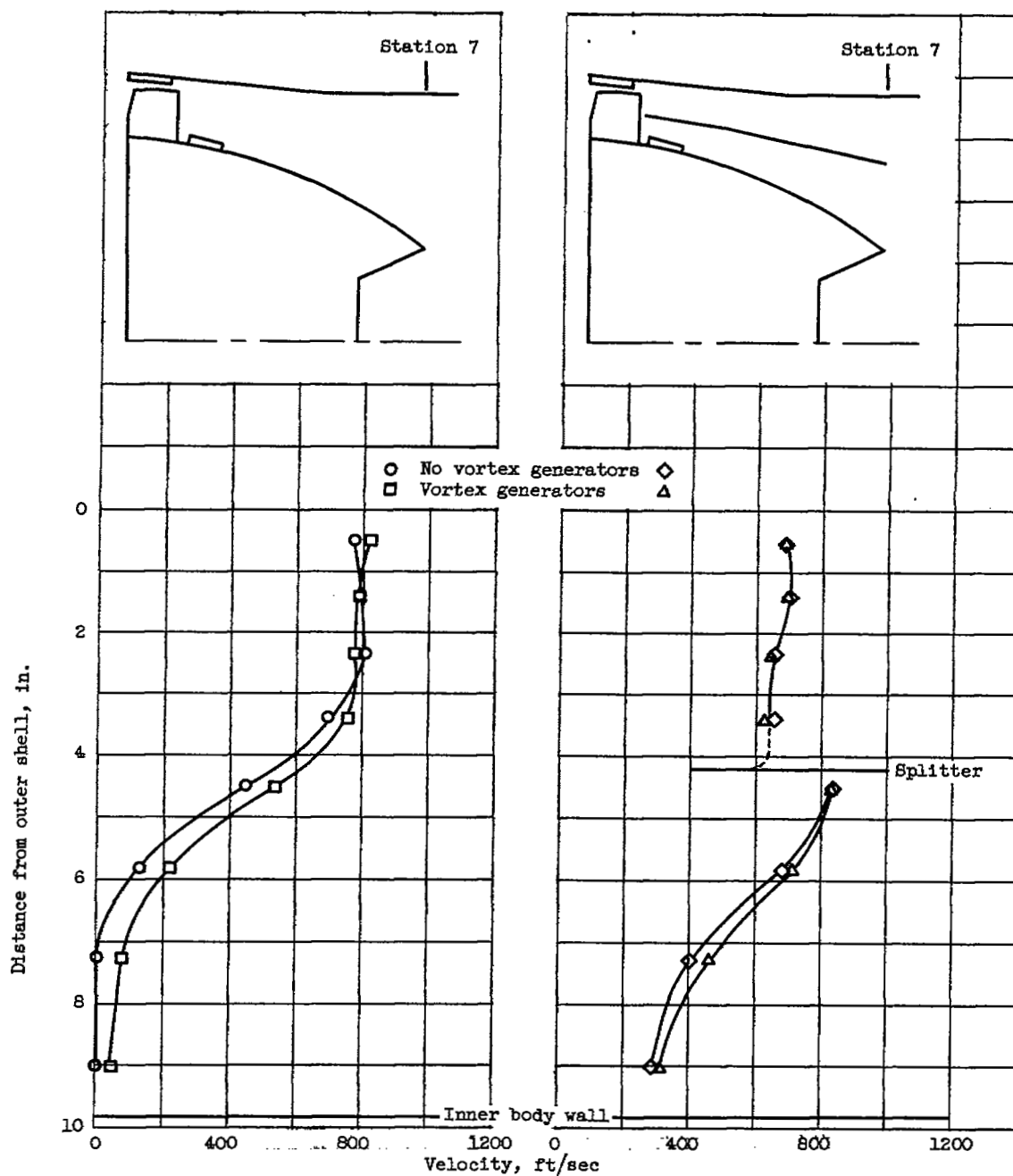


Figure 14. - Effect of splitters on velocity profile at station 7. Engine speed, 7900 rpm; inlet temperature, 100° F; exhaust gas temperature, 1250° F.



(a) Curved inner body.

(b) Curved inner body with splitter.

Figure 15. - Effect of vortex generators on velocity profile at station 7. Engine speed, 7900 rpm; inlet temperature, 100° F; exhaust gas temperature, 1250° F.

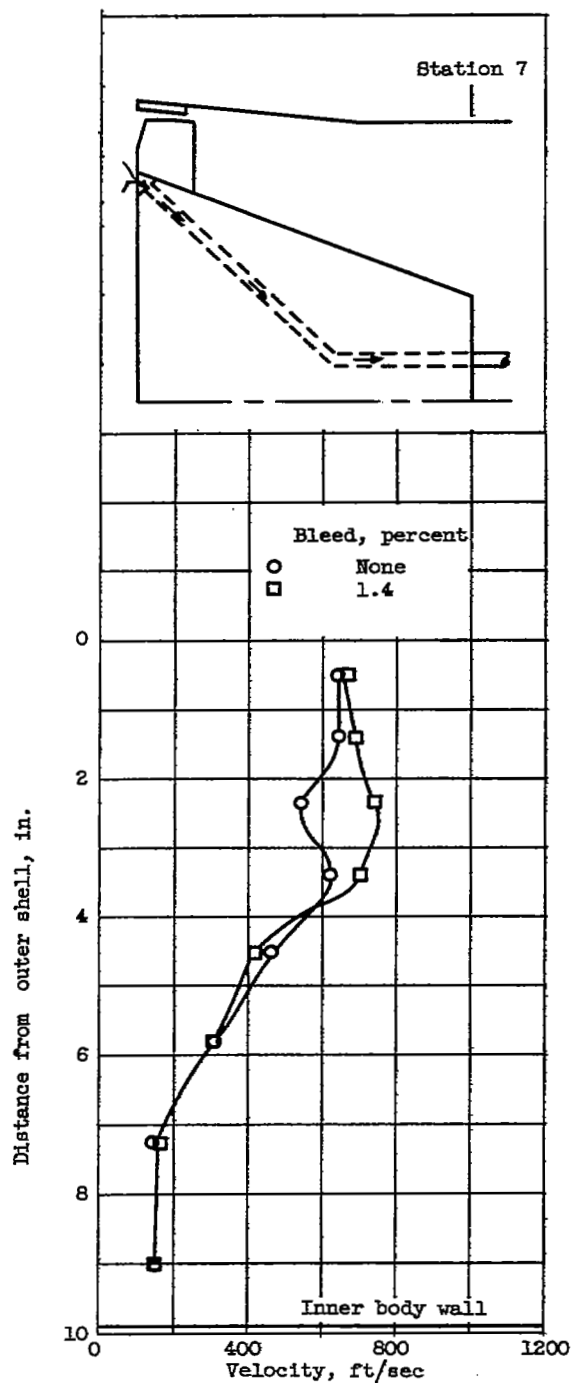


Figure 16. - Effect of turbine discharge bleed on velocity profile at station 7. Engine speed, 7900 rpm; inlet temperature, 100° F; exhaust gas temperature, 1250° F.



NASA Technical Library



3 1176 01435 3537

